HHS Public Access

Author manuscript

Mol Cancer Ther. Author manuscript; available in PMC 2018 September 01.

Published in final edited form as:

Mol Cancer Ther. 2017 September ; 16(9): 1819–1830. doi:10.1158/1535-7163.MCT-17-0013.

Combination treatment with orlistat-containing nanoparticles and taxanes is synergistic and enhances microtubule stability in taxane-resistant prostate cancer cells

Joshua J. Souchek[1], **Amanda L. Davis**[2], **Tanner K. Hill**[1], **Megan B. Holmes**[1], **Bowen Qi**[1], **Pankaj K. Singh**[3,4,5,6,7], **Steven J. Kridel**[2,8], and **Aaron M. Mohs**[1,4,7,*]

[1]Department of Pharmaceutical Sciences, University of Nebraska Medical Center, Omaha, Nebraska 68198, United States

[2]Department of Cancer Biology, Wake Forest University Health Sciences, Winston-Salem, North Carolina 27157, United States

[3]Eppley Institute for Research in Cancer and Allied Diseases, University of Nebraska Medical Center, Omaha, Nebraska 68198, United States

[4]Department of Biochemistry and Molecular Biology, University of Nebraska Medical Center, Omaha, Nebraska 68198, United States

[5]Department of Genetics, Cell Biology, and Anatomy, University of Nebraska Medical Center, Omaha, Nebraska 68198, United States

[6]Department of Pathology and Microbiology, University of Nebraska Medical Center, Omaha, Nebraska 68198, United States

[7]Fred and Pamela Buffett Cancer Center, University of Nebraska Medical Center, Omaha, Nebraska 68198, United States

[8]Wake Forest Comprehensive Cancer Center, Wake Forest University Health Sciences, Winston-Salem, North Carolina 27157, United States

Abstract

Taxane-based therapy provides a survival benefit in patients with metastatic prostate cancer, yet the median survival is less than 20 months in this setting due in part to taxane-associated resistance. Innovative strategies are required to overcome chemoresistance for improved patient survival. Here, NanoOrl, a new experimental nanoparticle formulation of the FDA-approved drug, orlistat, was investigated for its cytotoxicity in taxane-resistant prostate cancer utilizing two established taxane-resistant (TxR) cell lines. Orlistat is a weight loss drug that inhibits gastric lipases, but is also a potent inhibitor of fatty acid synthase (FASN), which is overexpressed in many types of cancer. NanoOrl was also investigated for its potential to synergize with taxanes in TxR cell lines. Both orlistat and NanoOrl synergistically inhibited cell viability when combined with paclitaxel, docetaxel, and cabazitaxel in PC3-TxR and DU145-TxR cells, yet these combinations were also additive in parental lines. We observed synergistic levels of apoptosis in

[*]**Correspondence to**: Aaron M. Mohs, Ph.D., Department of Pharmaceutical Sciences, University of Nebraska Medical Center, Eppley Cancer Institute, Room 4011, Omaha, NE 68198, aaron.mohs@unmc.edu.

TxR cells treated with NanoOrl and docetaxel in combination. Mechanistically, the synergy between orlistat and taxanes was independent of effects on the P-glycoprotein multidrug resistance protein, as determined by an efflux activity assay. On the other hand, immunoblot and immunofluorescence staining with an anti-detyrosinated tubulin antibody demonstrated that enhanced microtubule stability was induced by combined NanoOrl and docetaxel treatment in TxR cells. Furthermore, TxR cells exhibited higher lipid synthesis, as demonstrated by ^{14}C-choline incorporation, that was abrogated by NanoOrl. These results provide a strong rationale to assess the translational potential of NanoOrl to overcome taxane resistance.

Keywords

fatty acid synthase (FASN); orlistat; nanoparticle; hyaluronic acid; tubulin; chemoresistant; synergy; combination therapy

Introduction

Taxanes are a class of chemotherapeutics that bind to tubulin and stabilize microtubules. Several taxanes, including paclitaxel, albumin-bound paclitaxel (nab-paclitaxel), and docetaxel are approved for use alone or with other drugs for multiple cancers, including breast, ovarian, non-small cell lung cancer, pancreatic, among others (1–3). For patients with metastatic castration resistant prostate cancer (mCRPC), docetaxel is a standard treatment with a demonstrated survival benefit (4,5). Patients that initially respond to taxane-based therapy, however, invariably develop progressive disease. Consequently, a second-generation taxane, cabazitaxel, is approved for prostate cancer patients progressing after docetaxel-based chemotherapy (6). The structure of cabazitaxel confers a low affinity for the MDR1 (or P-glycoprotein [P-gp]; encoded by the ABCB1 gene) efflux pump, allowing for its use in taxane-resistant (TxR) cancer (7).

Several mechanisms have been associated with taxane resistance, including overexpression of drug efflux pumps, alterations in microtubules (i.e., mutations and isoform expression of tubulin), and changes in signaling pathways that enhance cell survival (7–9). A number of chemotherapeutics, including paclitaxel and docetaxel, are substrates for MDR1. In prostate cancer, MDR1 expression is directly correlated with tumor stage and grade (10). TxR prostate cancer cell lines have been reported to overexpress MDR1. For example, Takeda *et al.* (11) reported TxR-PC3 and TxR-DU145 cell lines by culturing parental cells with a stepwise concentration increase of paclitaxel. The resulting paclitaxel-resistant cells overexpressed MDR1 and were cross-resistant to docetaxel, estramustine phosphate, vinblastine, and doxorubicin (11).

Although rare, tubulin mutations found in human cancers are capable of conferring resistance to taxanes in a cell culture environment (12), and tubulin mutations at the drug binding site have been reported in TxR cell lines (13). High expression of the class III β-tubulin (βIII-tubulin) isotype has been associated with more aggressive and drug-resistant cancers (8,14). Expression of βIII-tubulin in prostate cancer tissues is predictive for poorer survival in docetaxel treated patients, and overexpression or knockdown of βIII-tubulin in prostate cancer cell lines modulated sensitivity to docetaxel (15). Similarly, expression of

βIII-tubulin in lung, breast, and ovarian tumor cells is associated with poorer survival in patients treated with taxanes (16–18). Altered expression of microtubule-associated proteins (MAPs) is also associated with changes in sensitivity to taxanes (8).

Fatty acid synthase (FASN) is the enzyme that produces *de novo* fatty acids (FAs). FASN expression and activity is increased in tumor cells and correlates with advanced tumor stage and poor patient prognosis (19,20). In prostate cancer, FASN mRNA is up-regulated in castration-resistant metastases compared to primary prostate tumors (21). Moreover, the FASN inhibitors cerulenin, C75, and C93 have been reported to enhance taxane sensitivity in resistant cancer cells (22–24). FASN-generated palmitate and other fatty acids, including palmitoleate and oleate, are found at higher levels in metastatic prostate cancer tissues compared to primary tumors (25). To that end, several FASN inhibitors are in development with a wide array of chemical structures (26–31). However, these compounds are either in early stages of preclinical development or are limited by severe side-effects. Alternatively, Kridel and colleagues discovered that orlistat is an effective FASN inhibitor (32–34), and binds to the thioesterase (TE) domain (33).

Orlistat is indicated as a lipase inhibitor, and is FDA-approved as a weight loss aid by blocking the absorption of dietary fat. A major challenge in the development of orlistat as a chemotherapeutic is its high hydrophobicity and poor bioavailability, which necessitate large doses to result in a tumor response in mice (32,35,36). To overcome these challenges, we recently reported the synthesis and characterization of a self-assembled nanoparticle (NP) formulation of orlistat, termed NanoOrl (37). Entrapment of orlistat in hyaluronic acid-derived NPs increases the solubility, stability, and efficacy of orlistat. NanoOrl was cytotoxic to LNCaP and PC3 prostate, and MDA-MB-231 breast cancer cell lines and inhibited the FASN-TE domain at a similar level as extracted stock orlistat, and lipid synthesis was reduced to similar levels in PC3 cells treated with either free orlistat or NanoOrl (37). The main objective of the current study was to investigate the potential of NanoOrl in taxane-resistant prostate cancer. Here, we determine the sensitivity of taxane-resistant cells to orlistat and NanoOrl, perform combination studies with multiple taxanes and NanoOrl, and examine potential synergistic mechanisms.

Materials and Methods

Materials

Paclitaxel, docetaxel, and cabazitaxel were purchased from LC Laboratories (Woburn, MA) and stock solutions were made in DMSO. Orlistat was purchased from Alfa Aesar (Ward Hill, MA) and stock solution was made in ethanol. Sodium hyaluronate (10 kDa) was purchased from Lifecore Biomedical (Chaska, MN). 1-Pyrenebutyric acid was obtained from Sigma-Aldrich (St. Louis, MO).

Preparation of NanoOrl

Synthesis of HA nanoparticles of orlistat (NanoOrl) was performed as described previously (37). Briefly, the hydrophobic ligand aminopropyl-1-pyrenebutanamide was conjugated to hyaluronic acid to drive self-assembly in aqueous solution (38). During self-assembly,

orlistat was entrapped in the hydrophobic domains of the nanoparticles. Nanoparticles were loaded with 20 wt% orlistat and had loading efficiency > 96% as determined by extraction from NanoOrl followed by HPLC quantification.

Cell lines and culture

PC3 and DU145 prostate cancer cell lines were obtained in 2013 from the American Type Culture Collection (Manassas, VA). The taxane-resistant (TxR) PC3-TxR and DU145-TxR cells were a kind gift from Dr. Ram Mahato (University of Nebraska Medical Center) in 2015, and were originally generated by Takeda *et al.* (11). PC3 and DU145 cells were maintained in RPMI 1640 medium supplemented with 10% fetal bovine serum, 100 I.U. penicillin, and 100 μg/mL streptomycin. PC3-TxR and DU145-TxR cells were maintained in RPMI 1640 medium containing 200 nM paclitaxel and supplementation described above. All cells were incubated at 37°C in a humidified incubator with 5% CO_2.

Cell viability assay

Cells (2000-3000 per well) were seeded in 96-well plates and allowed to adhere overnight. Cells were treated with indicated concentrations of orlistat, NanoOrl, empty NPs, paclitaxel, docetaxel, or cabazitaxel, or indicated combinations of drugs for 72 h. Concentrations of NanoOrl used for treatment are represented in the results as the equivalent concentration of orlistat. Cell viability was assessed by CCK-8 assay (Dojindo, Japan). Absorbance was read on a Synergy HTX Multi-Mode Reader (BioTek). Viability for treated cells was normalized to untreated cells on the same plate.

Analysis of synergy/antagonism from combination studies

To determine possible additive and synergistic effects when using combinations of a taxane with orlistat or NanoOrl, the data from cell viability assays was first analyzed using the freely available software, Combenefit (39), which simultaneously assesses synergy/antagonism using three published models (Highest single agent (HSA), Bliss, and Loewe). The software calculates a synergy score for each combination, where a positive score indicates synergy, a score of 0 is additive, and a negative score indicates antagonism. The “Contour” and “Matrix” views were selected as graphical outputs for the synergy distribution. The “Contour” view of synergy/antagonism is represented in the results section.

Results were also analyzed according to the Chou-Talalay model using the freely available CompuSyn software (ComboSyn, Inc., Paramus, NJ) developed by Chou and Martin (40). The software calculates the combination index (CI) for each drug combination, where a CI value < 1 indicates synergy, CI = 1 is additive and CI > 1 indicates antagonism. Data was uploaded manually for each combination, and the Log(CI) *vs.* Fa (Log of Combination Index *vs.* Fraction affected) plot was used for the results section.

Apoptosis assay

Cells (PC3-TxR = 9×10^4; DU145-TxR = 3×10^4 per well) were seeded in 12-well plates overnight, then treated with orlistat, NanoOrl, docetaxel, or in combination. After indicated treatment times, all cells from media, phosphate buffered saline (PBS) wash step, and trypsinization were combined, counted, and centrifuged. Cells were then stained with the

FITC Annexin V Apoptosis Detection Kit I (556547, BD Biosciences) per the manufacturer's recommendations. Stained cells were immediately analyzed using a BD LSRII flow cytometer in the Flow Cytometry Research Facility at UNMC.

Trypan blue exclusion assay

TxR cells were treated with or without Nano-Orl (12.5μM) and docetaxel (200 nM) for 24 hours (PC3-TxR) or 48 hours (DU145-TxR), then trypsinized and mixed 1:1 with trypan blue. Cells were counted in a hemocytometer using Invitrogen CountessTM Automated Cell Counter.

Western blot analysis

Cells were washed with PBS and lysed in radioimmuno precipitation assay (RIPA) lysis buffer containing protease inhibitors. Cell debris was removed by centrifugation at 13,000 rpm for 10 min and the supernatant was collected. Protein content was quantified using the Bio-Rad Protein Assay Dye (Bio-Rad Laboratories, Inc.). Equal amounts of total protein (20-30 μg) were separated by electrophoresis on SDS-PAGE gels and transferred to nitrocellulose membranes. The membranes were probed with primary antibodies against FASN (1:1000 dilution, 3180S, Cell Signaling Technology), MDR-1 (1:500, sc-55510, Santa Cruz Biotechnology), detyrosinated tubulin (1:750, AB3201, EMD Millipore), alpha-tubulin (1:1000, MABT205, EMD Millipore), cleaved PARP (1:2000, #9546, Cell Signaling Technology), phosphorylated-ERK (Thr202/Tyr204) (1:1000, #9101, Cell Signaling Technology), total-ERK (1:2000, #4696, Cell Signaling Technology), phosphorylated-Akt (Ser473) (1:1000, #9271, Cell Signaling Technology), total-Akt (1:1000, #9272, Cell Signaling Technology), cleaved Caspase 3 (1:500, #9664, Cell Signaling Technology), beta-tubulin (1:100, Clone E7, developed by Michael Klymkowsky was obtained from the Developmental Studies Hybridoma Bank, Iowa City, IA), and actin (1:800, JLA20, developed by J. J.-C. Lin was obtained from the Developmental Studies Hybridoma Bank, Iowa City, IA) in TBS with 5% nonfat milk and 0.1% Tween-20 with gentle agitation overnight at 4°C. HRP-conjugated secondary antibodies (1:5000 dilution) were incubated in TBS with 5% nonfat milk and 0.1% Tween-20 with gentle agitation for 1 h at room temperature. Pierce ECL Western Blotting Substrate (Thermo Scientific) was added to the membranes and then exposed to ECL-sensitive X-ray film (Phenix Research Products). The films were developed and then digitally scanned. Quantification of bands was analyzed with Image J and figures were assembled using Adobe Illustrator.

^{14}C-choline incorporation into lipid

Cells were seeded in 24-well plates at 7×10^4 cells/well. After 24 h, the cells were treated with vehicle (empty NPs) or NanoOrl (50μM) for 24 h. Cells were pulsed with 1 μCi [methyl-^{14}C]choline chloride (ARC 0208, American Radiolabeled Chemicals, Inc., St. Louis, MO) for 2 h to label newly synthesized lipid. Cells were then washed with PBS and lysed in hypotonic buffer (1mM dithiothreitol (DTT), 1mM ethylenediaminetetraacetic acid (EDTA), 20mM Tris, pH 7.5) for 30 minutes at room temperature. Lipids were extracted with chloroform:methanol (2:1 v/v). ^{14}C-Choline incorporation was quantified by scintillation counting. Results were normalized to protein concentration as determined by Lowry assay.

Multidrug Resistance Assay

The activity of MDR1 in cells was characterized with the Vybrant Multidrug Resistance Assay Kit (V-13180, Molecular Probes), which evaluates the fluorescence of calcein-acetoxymethyl ester (AM) accumulation in the cells. Briefly, cells were seeded in 96-well plates overnight, then treated with orlistat, NanoOrl, empty nanoparticles, or the MDR1 inhibitor verapamil as a control. After indicated treatment times, the cells were incubated in calcein AM (final concentration of 0.25 μM) for 30 min. The cells were washed three times with PBS and the cell fluorescence was measured with a Synergy HTX Multi-Mode Reader (BioTek) equipped with 485/20 nm and 528/20 nm excitation and emission filters, respectively.

Immunofluorescence microscopy

Cells were seeded (1×10^4 per well) in 96-well, black-walled, clear bottom plates in 200 μL of media overnight. Cells were treated as specified for 2.5 h, then were fixed in 150 μL of ice cold methanol for 10 min. The methanol was removed and 150 μL of wash buffer (0.15% Triton X-100 in PBS) was dispensed for 10 min and then removed. 100 μL of blocking solution (1% BSA, 0.1% Tween in PBS) was dispensed and incubated for 30 minutes at room temperature. 50 μL of anti-detyrosinated tubulin (Millipore Ab3201) at 1:100 in blocking solution was incubated for 1 h at room temperature. Wells were washed 3 times with 100 μL of wash buffer, each time for 3 minutes, and then incubated with 75 μL of FITC-conjugated anti-rabbit secondary antibody (Millipore AP132F) at 1:100 in blocking solution for 1 h at room temperature. Wells were again washed 3 times with 100 μL of wash buffer, each time for 3 minutes. The nuclear stain DAPI, diluted in ultrapure water, was added and left for 5 minutes before aspirating, followed by washing for 3 times with 100 μL of ultra-pure water, each time for 3 minutes. Finally, 200 μL of PBS was added to each well. Images were taken on an Olympus IX73 inverted microscope. Images were analyzed with Image J (NIH) using identical processing parameters.

Results

Taxane resistant (TxR) prostate cancer cells have increased lipid synthesis

Immunoblot detection demonstrates that PC3-TxR cells had similar levels of FASN protein expression, while DU145-TxR had marginally decreased FASN, compared to parent lines (Fig. 1A). Functionally, TxR cells incorporated ^{14}C-choline into lipid at a higher level than parental cells, with PC3-TxR having 300% higher lipid synthesis than PC3 parental cells and DU145-TxR cells having 50% higher lipid synthesis than DU145 parental cells (Fig. 1B). Choline can be converted to phosphatidylcholine, the predominant phospholipid (>50%) in most mammalian membranes (41) and phosphatidylcholine synthesis requires FASN-generated fatty acids. Importantly, treatment with NanoOrl significantly lowered ^{14}C-choline incorporation into lipid in all four cell lines. While NanoOrl treatment reduced ^{14}C-choline incorporation by 2.9-fold in PC3 cells, it was decreased by 6.4-fold in PC3-TxR cells. Similarly, ^{14}C-choline incorporation was reduced by 3.3-fold in DU145 cells, and was decreased by 5.5-fold in DU145-TxR cells.

Confirmation of taxane resistance and sensitivity of TxR cells to NanoOrl

Resistance to paclitaxel and docetaxel was confirmed, with PC3-TxR cells 153-fold more resistant to paclitaxel and 108-fold more resistant to docetaxel compared to parent PC3 cells (Fig. 1C and D, Table 1). DU145-TxR cells were 500-fold and 337-fold more resistant to paclitaxel and docetaxel, respectively, compared to parent DU145 cells (Fig. 1C and D, Table 1). PC3-TxR and DU145-TxR cells were 12-fold and 39-fold more resistant to the second-generation taxane cabazitaxel, respectively, compared to parent cells (Fig. 1E, Table 1). Interestingly, PC3-TxR cells were 1.5-fold and 2.3-fold more sensitive to free orlistat and NanoOrl, respectively, while DU145-TxR were 1.3-fold more sensitive to NanoOrl (Fig. 1F and G, Table 1). Treatment of cells with the empty HA-PBA nanoparticles (992 μg/mL), which is the equivalent concentration to the highest NanoOrl concentration, did not have marked effect on cell viability (Fig. 1H).

NanoOrl synergizes with taxanes in TxR prostate cancer cells

Because FASN inhibitors can sensitize tumor cells to various chemotherapeutics, including taxanes, the potential for synergy between taxanes and orlistat or NanoOrl was performed in TxR lines. Calculating the half maximal inhibitory concentration (IC_{50}) of cell viability of each taxane at different NanoOrl concentrations, the IC_{50} was independent of NanoOrl concentration in parent cells (Fig. 2). For example, the IC_{50} for paclitaxel, docetaxel, and cabazitaxel in PC3 cells was 6.1 nM, 3.6 nM, and 1.2 nM, and decreased slightly to 4.4 nM, 2.2 nM, and 0.63 nM with 25 μM NanoOrl treatment, respectively. For DU145 cells, the IC_{50} for paclitaxel, docetaxel, and cabazitaxel was 4.9 nM, 2.7 nM, and 0.79 nM and decreased to 3.9 nM, 1.9 nM, and 0.41 nM with 25 μM NanoOrl treatment, respectively. Conversely, the IC_{50} for each taxane decreased markedly with increasing concentration of NanoOrl in TxR cells (Fig. 2). For example, the paclitaxel IC_{50} in PC3-TxR cells decreased 19-fold, decreasing from 0.94 μM to 50 nM with 25 μM NanoOrl treatment. The docetaxel IC_{50} in PC3-TxR cells decreased 13-fold from 380 nM to 25 nM with 12.5 μM NanoOrl treatment, and the cabazitaxel IC_{50} in PC3-TxR cells decreased 12-fold from 15 nM to 1.2 nM with 25 μM NanoOrl treatment, which is approaching the IC_{50} of the parent line. Similarly, for DU145-TxR cells, the IC_{50} for paclitaxel, docetaxel, and cabazitaxel was 2.4 μM, 0.91 μM, and 30 nM and decreased to 0.8 μM, 0.15 μM, and 10 nM with 25 μM NanoOrl treatment, respectively. Shifts to the left (decreasing IC_{50}) in the dose response curves were clearly visible for TxR cells, but not for parent cells (Supplementary Fig. S1).

The synergy of drug combinations using data from the cell viability assays was first analyzed using Combenefit (39). The contour plot of synergy/antagonism with the Bliss model is shown in Fig 3, while the Loewe and HSA are shown in Supplementary Figs. S2 and S3. These plots indicate strong synergy between orlistat and NanoOrl with all three taxanes in the PC3-TxR and DU145-TxR cells, while additive scores were seen in parental PC3 or DU145 cells (Fig. 3A). Synergy scores (the difference between the predicted additivity and the observed viability, with positive scores being synergistic and negative scores antagonistic) for the Bliss model reached over 50 in areas in all five different combinations in PC3-TxR cells, and were over 25 for DU145-TxR. For example, PC3-TxR cells had 81.6% viability when treated for 72 h with 200 nM docetaxel (relative to untreated control), 75.6% viability when treated with 6.25 μM NanoOrl, and 6.0% viability when

treated with the combination of 200 nM docetaxel plus 6.25 μM NanoOrl. Using the Bliss model, the predicted additive viability is 61.8%. Thus, the synergy score was calculated to be 61.8 – 6 = 55.8 (Fig. 3B). In contrast, the synergy score for PC3 cells treated with combination of 1 nM docetaxel plus 25 μM NanoOrl had a low synergy score of 5.5 (Fig. 3C). Similar trends in synergism were seen with the Loewe and HSA models, although synergy scores were lower for the most stringent Loewe model, and higher for the least stringent HSA model (Supplementary Fig. S2 and S3, respectively).

CompuSyn (Chou-Talalay model (40)) results showed that a higher percentage of combinations of orlistat or NanoOrl plus taxanes were synergistic (CI<1) in the TxR cells (67-98% for PC3-TxR and 67-83% for DU145-TxR) compared to the parent lines, demonstrating that this software also shows synergy in TxR cells (Fig. 3D). The parent cells had a small majority of combinations with CI<1 (55–69% for PC3 and 60–71% for DU145), but most combinations were close to additive. For comparison, the examples given above of PC3-TxR cells treated with the combination of 200 nM docetaxel plus 6.25 μM NanoOrl had strong synergism (CI = 0.21), while PC3 cells treated with the combination of 1 nM docetaxel plus 25 μM NanoOrl had slight synergism (CI = 0.87).

NanoOrl plus docetaxel combination induces apoptosis

Apoptosis of TxR cells was assessed by Annexin V-FITC and propidium iodide staining with flow cytometry using doses of orlistat or NanoOrl with docetaxel that had high synergy score from the synergy analyses. We observed that the combination treatments had significantly higher apoptosis than either treatment alone ($p<0.0001$). In PC3-TxR cells, single treatment with orlistat or NanoOrl (12.5 μM), or docetaxel (200 nM) did not significantly increase the percentage of early apoptotic (Annexin V+/PI-; Fig. 4A and C) or late apoptotic/necrotic (Annexin V+/PI+; Fig. 4A and D) cells over basal levels. On the other hand, a 24 h treatment with either combination of orlistat plus docetaxel, or NanoOrl plus docetaxel, significantly increased the percentage of both early and late apoptotic/necrotic cells, with total Annexin V+ levels reaching 43% and 53%, respectively. The percentage of apoptotic cells in DU145-TxR cells was also significantly increased compared to single drug treatment, but was not as robust as PC3-TxR cells. The total Annexin V+ levels reach 20% and 19% after a 48 h treatment with a combination of orlistat (12.5 μM) plus docetaxel (500 nM), or NanoOrl (12.5 μM) plus docetaxel (500 nM), respectively (Fig. 4B, E, and F). The morphology of the cells treated with sub-IC_{50} concentrations of either docetaxel, NanoOrl, or orlistat alone appeared similar to untreated cells. However, in the combination treatment, many cells could be seen detached from the plastic or rounded up and loosely attached to the plastic (Supplementary Fig. S4).

Cell death was also assessed by trypan blue assay. A significant three-fold increase in the percentage of trypan blue-positive cells was seen in PC3-TxR cells treated with the combination of docetaxel (200 nM) and NanoOrl (12.5 μM) (Fig. 4G), while a two-fold increase was seen in DU145-TxR cells treated with the same combination (Fig. 4I). Apoptotic signaling was also confirmed in PC3-TxR cells, with levels of cleaved PARP and cleaved caspase 3 detectable only in the combination treatment (Fig. 4H). On the other hand, cleaved PARP and cleaved caspase 3 were not detectable in DU145-TxR cells treated with

docetaxel (200 nM) and NanoOrl (12.5 μM) (Fig. 4J), suggesting that death occurred through a non-canonical mechanism. Thus, it appears that the combination treatments effectively kill cells through multiple mechanisms.

While phosphorylation of ERK 1/2 and subsequent activation of downstream targets is often associated with cell survival, activation of this pathway is also implicated in apoptotic signaling (42–44). Western blot analysis of PC3-TxR cells showed increased phosphorylated ERK 1/2 (Thr202/Tyr204) in response to NanoOrl treatment and combination NanoOrl/Docetaxel treatment (Fig. 4H). Because increased phosphorylated ERK 1/2 is seen in response to both a treatment that did result in increased cell death and a treatment that did not result in increased cell death, it seems that the apoptosis seen with combination treatment in the PC3-TxR cells is achieved in an ERK 1/2 independent manner. Moreover, while DU145-TxR cells seem to express more phosphorylated ERK 1/2 than PC3-TxR cells (Fig. 4H and J), a similar level of phosphorylated ERK 1/2 is seen across treatment conditions with no notable change with combination NanoOrl/Docetaxel treatment, yet resulted in an increased percentage of cells positive for trypan blue (Fig. 4I). This further suggests that cell survival or cell death in these experiments is achieved regardless of ERK 1/2 activation. No effect was seen in phosphorylated-Akt (Ser473) levels across treatment conditions (Fig. 4H and J).

Orlistat and NanoOrl do not affect MDR1 activity in TxR prostate cancer cells

Because MDR1 is associated with the TxR phenotype of these cells, we tested whether orlistat or NanoOrl affected MDR1 activity. We confirmed that both PC3-TxR and DU145-TxR cells had increased MDR1 expression by western blot (Fig. 1A). Calcein AM efflux assays confirmed that MDR1 activity was elevated (i.e., lower cell fluorescence) in TxR cells relative to the parent lines, however, MDR1 activity was not affected by orlistat or NanoOrl treatment at concentrations up to 50 μM in either TxR cell line, or by empty NPs (Fig. 5A and B). The MDR1 inhibitor, verapamil, was used as a positive control.

Combination of NanoOrl and docetaxel stabilizes microtubules in TxR cells

The PC3-TxR and DU145-TxR cells overexpress several β-tubulin isoforms (11,45). We observed that DU145-TxR cells had 1.78-fold increased expression of total β-tubulin (Fig. 1A). We next wanted to determine if the combination of NanoOrl and docetaxel functionally affected microtubule stability. Intriguingly, immunoblot of whole cell lysates with an anti-detyrosinated α-tubulin (also known as glu-tubulin) antibody, a marker of stabilized microtubules (46–48), demonstrated that the combination of NanoOrl and docetaxel increased microtubule stability in PC3-TxR and in DU145-TxR cells above that seen with docetaxel alone (Fig. 5C and D). The ratio of detyrosinated-tubulin to alpha-tubulin was nearly two-fold higher in PC3-TxR cells and 2.7- to 4-fold higher in DU145-TxR cells treated with the combination compared to docetaxel alone. Further, immunofluorescent staining with the anti-detyrosinated α-tubulin antibody demonstrated that docetaxel increased microtubule stability in PC3 cells as expected (Supplementary Fig. S5A). The level of detyrosinated tubulin were drastically reduced in PC3-TxR cells compared to PC3 cells when treated with docetaxel alone (Fig. 5E and F, quantified in Fig. 5H and I). Microtubule stability in PC3-TxR cells was increased by the combination of NanoOrl and

docetaxel above that seen with docetaxel alone ($p < 0.0001$) (Fig. 5F and G, quantified in Fig. 5I), although not to the level seen in PC3 cells treated with docetaxel (Fig. 5E and H). On the other hand, the combination of NanoOrl with docetaxel did not enhance docetaxel-induced microtubule stability in PC3 cells (Fig. 5H, Supplementary Fig. S5A). Increased microtubule stability was not observed when using NanoOrl alone up to 100 μM (Supplementary Fig. S5B). These results suggest that the synergy between NanoOrl and taxanes in TxR cells may be linked to effects on microtubule stability.

Discussion

In this study, taxane resistance was overcome with orlistat, an off-the-shelf, FDA-approved pharmaceutical, and with a recently reported nanoparticle formulation of orlistat, NanoOrl (37). The combination of orlistat or NanoOrl with taxanes showed robust synergy with four models (from two separate software packages) of synergy analysis. While the FASN inhibitors cerulenin, C75, or C93 have been reported to enhance taxane sensitivity in resistant cancer cells (22–24), this study is the first, to our knowledge, to show that orlistat synergizes with taxanes in cancer cells. Treatment with NanoOrl overcame resistance to first-generation taxanes, including docetaxel, which is approved as first-line therapy in mCRPC, and to the second-generation taxane, cabazitaxel. Cabazitaxel is designed to have low affinity for MDR1. We expected TxR cells to have the same IC_{50} of cabazitaxel as parent cells. However, the TxR cells were still one order of magnitude more resistant to cabazitaxel compared to parent cells (Table 1), suggesting that other mechanisms of taxane resistance besides MDR1 activity exist in these cells. Given that NanoOrl did not affect MDR1 activity (Fig. 5A and B) and that synergy still occurred with a taxane that can evade MDR1 related efflux, our data suggests that synergy between orlistat and taxanes is independent of MDR1 function. Instead, the synergy reported here is associated with increased microtubule stability (Fig. 5C–I), suggesting a potential new mechanism to overcome this drug resistance.

While it remains unclear how microtubule stability is increased by the combination of NanoOrl and docetaxel in TxR cells, several studies from the literature point to potential molecular mechanisms. A recent report using a clickable-analog of orlistat showed that the analog does bind to β-tubulin, but this study did not show the functional consequence of this binding (49). Consequently, we hypothesized that beyond its ability to inhibit FASN, orlistat may also directly affect microtubule stability. However, we did not observe increased microtubule stability in our immunoblot (Fig. 5 C and D) or immunofluorescence analyses using doses of NanoOrl up to 100 μM (Supplementary Fig. S5B). Tubulin is also post-translationally modified with palmitate, and palmitoylated-tubulin is found along microtubule tracks and also partially associated with the plasma membrane (50). Interestingly, it has been reported that FASN is required for palmitoylation of specific targets in cancer (51,52). Thus, the inhibition of FASN and palmitate production by orlistat and NanoOrl may affect post-translational modification of tubulin, and thus affect microtubule stability. A recent paper using the FASN inhibitors TVB-3166 and TVB-3664 showed that FASN inhibition reduced tubulin palmitoylation and disrupted microtubule organization in tumor cells (53). The authors showed that FASN inhibition combined with taxane treatment enhances inhibition of *in vitro* tumor cell growth. The authors also showed that FASN

inhibition does not affect intracellular paclitaxel concentrations, although these studies were not examined in TxR cells. We hypothesize that orlistat and NanoOrl could similarly reduce tubulin palmitoylation and may disrupt microtubule organization, but our data shows that orlistat and NanoOrl alone do not affect microtubule stability, using detyrosinated tubulin levels as a biomarker for stabilized microtubules. This suggests that FASN inhibition alone may disrupt the localization of tubulin and disrupt microtubule organization, but may not stabilize microtubules.

The increased activity of the fatty acid synthesis pathway in TxR cells could also provide additional mechanistic insights. Both TxR lines had significantly increased incorporation of ^{14}C-choline into lipids, while DU145-TxR cells had a smaller increase compared to the PC3-TxR line (Fig. 1B). This difference may explain why PC3-TxR cells have increased sensitivity to orlistat and NanoOrl relative to the DU145-TxR cells (Table 1 and Fig. 1F and G), and may explain why the level of synergy in viability studies (Fig. 3A) and the percentage of apoptotic cells in DU145-TxR cells upon combination treatment was not as robust as PC3-TxR cells (Fig. 4A–F). Overall, both TxR cell lines had increased fatty acid synthesis compared to parental cell lines and fatty acid synthesis was more robustly inhibited by NanoOrl treatment in the TxR cells compared to parent cells (Fig. 1B). This suggests that the level of synergy was related to increased lipid synthesis.

It should be noted that the Combenefit software gave a warning in a few of our analyses for low goodness of fit for single agent dose-response curves. Decreased goodness of fit could be due to a dose-response that could not be fit by the traditional Hill model, which is used to fit single-agent data values to calculate synergy. For example, overestimation of synergy was observed in PC3-TxR cells with select combinations of orlistat and paclitaxel (Supplementary Fig. S6), while an underestimation of synergy was observed in DU145-TxR cells with select combinations of NanoOrl and cabazitaxel (Supplementary Fig. S7). Nevertheless, individual calculations (thus, not reliant on fitting with the Hill model) still result in a highly synergistic interaction (Supplementary Fig. S6).

NP formulations of orlistat show promise for improved cytotoxicity and delivery to tumors as demonstrated by us (37) and others (54–56). Paulmurugan *et al.* showed a 70% tumor volume reduction in MDA-MB-231 xenografts using folate receptor-targeted, 2-hydroxyethylacrylate and 2-ethylhexylacrylate-based copolymer micellar nanoparticles (54). Preclinical *in vivo* studies have shown anti-tumor efficacy of orlistat treatment with nearly a 3 order of magnitude range of total dose administered, from two doses of 2 mg/kg BW orlistat to 240 mg/kg/day for three weeks (32,35,36,54). Therefore, a systematic determination of efficacious *in vivo* dose is needed for NanoOrl used alone or in combination with taxanes. Besides taxanes, NP formulations of orlistat may be used in combination with other chemotherapy classes, as inhibition of FASN can sensitize pancreatic or breast cancer cells to gemcitabine or 5-fluorouracil (57,58). NP formulations of orlistat may also be used with radiation, as others have shown that inhibition of FASN can sensitize head and neck squamous or prostate cancer cells to radiation (59,60). Given the strong synergy between NanoOrl and taxanes in taxane-resistant prostate cancer cells, our data warrant the further evaluation of NanoOrl for cancer therapy either alone or in combination with taxanes.

Supplementary Material

Refer to Web version on PubMed Central for supplementary material.

Acknowledgments

We thank Victoria B. Smith and Samantha D. Wall for technical assistance in the UNMC Flow Cytometry Research Facility.

Financial Support: National Institute of General Medical Sciences (P20 GM103480), the National Cancer Institute (R01 CA163649, R01 CA210439, R01 CA216853, and 2P50 CA127297), the Fred and Pamela Buffett Cancer Center at UNMC (P30 CA036727), and the Comprehensive Cancer Center of Wake Forest University (P30 CA012197).

References

1. Von Hoff DD, Ervin T, Arena FP, Chiorean EG, Infante J, Moore M, et al. Increased survival in pancreatic cancer with nab-paclitaxel plus gemcitabine. N Engl J Med. 2013; 369:1691–703. [PubMed: 24131140]
2. Gradishar WJ, Tjulandin S, Davidson N, Shaw H, Desai N, Bhar P, et al. Phase III trial of nanoparticle albumin-bound paclitaxel compared with polyethylated castor oil-based paclitaxel in women with breast cancer. J Clin Oncol. 2005; 23:7794–803. [PubMed: 16172456]
3. Socinski MA, Bondarenko I, Karaseva NA, Makhson AM, Vynnychenko I, Okamoto I, et al. Weekly nab-paclitaxel in combination with carboplatin versus solvent-based paclitaxel plus carboplatin as first-line therapy in patients with advanced non-small-cell lung cancer: final results of a phase III trial. J Clin Oncol. 2012; 30:2055–62. [PubMed: 22547591]
4. Tannock IF, de Wit R, Berry WR, Horti J, Pluzanska A, Chi KN, et al. Docetaxel plus prednisone or mitoxantrone plus prednisone for advanced prostate cancer. N Engl J Med. 2004; 351:1502–12. [PubMed: 15470213]
5. Petrylak DP, Tangen CM, Hussain MHA, Lara PN, Jones JA, Taplin ME, et al. Docetaxel and estramustine compared with mitoxantrone and prednisone for advanced refractory prostate cancer. N Engl J Med. 2004; 351:1513–20. [PubMed: 15470214]
6. De Bono JS, Oudard S, Ozguroglu M, Hansen S, MacHiels JP, Kocak I, et al. Prednisone plus cabazitaxel or mitoxantrone for metastatic castration-resistant prostate cancer progressing after docetaxel treatment: A randomised open-label trial. Lancet. 2010; 376:1147–54. [PubMed: 20888992]
7. Mellado B, Jimenez N, Marin-Aguilera M, Reig O. Diving Into Cabazitaxel's Mode of Action: More Than a Taxane for the Treatment of Castration-Resistant Prostate Cancer Patients. Clin Genitourin Cancer. 2016; 14:265–70. [PubMed: 26827258]
8. Kavallaris M. Microtubules and resistance to tubulin-binding agents. Nat Rev Cancer. 2010; 10:194–204. [PubMed: 20147901]
9. Antonarakis ES, Armstrong AJ. Evolving standards in the treatment of docetaxel-refractory castration-resistant prostate cancer. Prostate Cancer Prostatic Dis. 2011; 14:192–205. [PubMed: 21577234]
10. Bhangal G, Halford S, Wang J, Roylance R, Shah R, Waxman J. Expression of the multidrug resistance gene in human prostate cancer. Urol Oncol. 2000; 5:118–21. [PubMed: 10765019]
11. Takeda M, Mizokami A, Mamiya K, Li YQ, Zhang J, Keller ET, et al. The establishment of two paclitaxel-resistant prostate cancer cell lines and the mechanisms of paclitaxel resistance with two cell lines. Prostate. 2007; 67:955–67. [PubMed: 17440963]
12. Yin S, Bhattacharya R, Cabral F. Human mutations that confer paclitaxel resistance. Mol Cancer Ther. 2010; 9:327–35. [PubMed: 20103599]
13. Giannakakou P, Sackett DL, Kang YK, Zhan Z, Buters JTM, Fojo T, et al. Paclitaxel-resistant human ovarian cancer cells have mutant β-tubulins that exhibit impaired paclitaxel-driven polymerization. J Biol Chem. 1997; 272:17118–25. [PubMed: 9202030]

14. Sève P, Dumontet C. Is class III beta-tubulin a predictive factor in patients receiving tubulin-binding agents? Lancet Oncol. 2008; 9:168–75. [PubMed: 18237851]
15. Ploussard G, Terry S, Maillé P, Allory Y, Sirab N, Kheuang L, et al. Class III β-tubulin expression predicts prostate tumor aggressiveness and patient response to docetaxel-based chemotherapy. Cancer Res. 2010; 70:9253–64. [PubMed: 21045157]
16. Sève P, Mackey J, Isaac S, Trédan O, Souquet P-J, Pérol M, et al. Class III β-tubulin expression in tumor cells predicts response and outcome in patients with non-small cell lung cancer receiving paclitaxel. Mol Cancer Ther. 2005; 4:2001–7. [PubMed: 16373715]
17. Galmarini CM, Treilleux I, Cardoso F, Bernard-Marty C, Durbecq V, Gancberg D, et al. Class III β-tubulin isotype predicts response in advanced breast cancer patients randomly treated either with single-agent doxorubicin or docetaxel. Clin Cancer Res. 2008; 14:4511–6. [PubMed: 18628466]
18. Ferrandina G, Zannoni GF, Martinelli E, Paglia A, Gallotta V, Mozzetti S, et al. Class III beta-tubulin overexpression is a marker of poor clinical outcome in advanced ovarian cancer patients. Clin Cancer Res. 2006; 12:2774–9. [PubMed: 16675570]
19. Kuhajda FP. Fatty Acid Synthase and Cancer: New Application of an Old Pathway. Cancer Res. 2006; 66:5977–80. [PubMed: 16778164]
20. Kuhajda FP. Fatty-acid synthase and human cancer: new perspectives on its role in tumor biology. Nutrition. 2000; 16:202–8. [PubMed: 10705076]
21. Montgomery RB, Mostaghel EA, Vessella R, Hess DL, Kalhorn TF, Higano CS, et al. Maintenance of intratumoral androgens in metastatic prostate cancer: a mechanism for castration-resistant tumor growth. Cancer Res. 2008; 68:4447–54. [PubMed: 18519708]
22. Menendez JA, Lupu R, Colomer R. Inhibition of tumor-associated fatty acid synthase hyperactivity induces synergistic chemosensitization of HER -2/neu -overexpressing human breast cancer cells to docetaxel (taxotere). Breast Cancer Res Treat. 2004; 84:183–95. [PubMed: 14999148]
23. Menendez JA, Vellon L, Colomer R, Lupu R. Pharmacological and small interference RNA-mediated inhibition of breast cancer-associated fatty acid synthase (oncogenic antigen-519) synergistically enhances Taxol (paclitaxel)-induced cytotoxicity. Int J Cancer. 2005; 115:19–35. [PubMed: 15657900]
24. Meena AS, Sharma A, Kumari R, Mohammad N, Singh SV, Bhat MK. Inherent and acquired resistance to paclitaxel in hepatocellular carcinoma: molecular events involved. PLoS One. 2013; 8:e61524. [PubMed: 23613870]
25. Sreekumar A, Poisson LM, Rajendiran TM, Khan AP, Cao Q, Yu J, et al. Metabolomic profiles delineate potential role for sarcosine in prostate cancer progression. Nature. 2009; 457:910–4. [PubMed: 19212411]
26. Zhou W, Han WF, Landree LE, Thupari JN, Pinn ML, Bililign T, et al. Fatty acid synthase inhibition activates AMP-activated protein kinase in SKOV3 human ovarian cancer cells. Cancer Res. 2007; 67:2964–71. [PubMed: 17409402]
27. Zhou W, Simpson PJ, McFadden JM, Townsend CA, Medghalchi SM, Vadlamudi A, et al. Fatty acid synthase inhibition triggers apoptosis during S phase in human cancer cells. Cancer Res. 2003; 63:7330–7. [PubMed: 14612531]
28. Turrado C, Puig T, García-Cárceles J, Artola M, Benhamú B, Ortega-Gutiérrez S, et al. New Synthetic Inhibitors of Fatty Acid Synthase with Anticancer Activity. J Med Chem American Chemical Society. 2012; 55:5013–23.
29. Puig T, Aguilar H, Cufí S, Oliveras G, Turrado C, Ortega-Gutiérrez S, et al. A novel inhibitor of fatty acid synthase shows activity against HER2+ breast cancer xenografts and is active in anti-HER2 drug-resistant cell lines. Breast Cancer Res BioMed Central Ltd. 2011; 13:R131.
30. Puig T, Turrado C, Benhamú B, Aguilar H, Relat J, Ortega-Gutiérrez S, et al. Novel Inhibitors of Fatty Acid Synthase with Anticancer Activity. Clin Cancer Res. 2009; 15:7608–15. [PubMed: 20008854]
31. Selvendiran K, Ahmed S, Dayton A, Ravi Y, Kuppusamy ML, Bratasz A, et al. HO-3867, a synthetic compound, inhibits the migration and invasion of ovarian carcinoma cells through downregulation of fatty acid synthase and focal adhesion kinase. Mol Cancer Res. 2010; 8:1188–97. [PubMed: 20713491]

32. Kridel SJ, Axelrod F, Rozenkrantz N, Smith JW. Orlistat is a novel inhibitor of fatty acid synthase with antitumor activity. Cancer Res. 2004; 64:2070–5. [PubMed: 15026345]
33. Pemble CW, Johnson LC, Kridel SJ, Lowther WT. Crystal structure of the thioesterase domain of human fatty acid synthase inhibited by Orlistat. Nat Struct Mol Biol. 2007; 14:704–9. [PubMed: 17618296]
34. Little JL, Wheeler FB, Koumenis C, Kridel SJ. Disruption of crosstalk between the fatty acid synthesis and proteasome pathways enhances unfolded protein response signaling and cell death. Mol Cancer Ther. 2008; 7:3816–24. [PubMed: 19074856]
35. Yoshii Y, Furukawa T, Oyama N, Hasegawa Y, Kiyono Y, Nishii R, et al. Fatty Acid Synthase Is a Key *Target* in Multiple Essential Tumor Functions of Prostate Cancer: Uptake of Radiolabeled Acetate as a Predictor of the Targeted Therapy Outcome. PLoS One. 2013; 8:e64570. [PubMed: 23741342]
36. Carvalho MA, Zecchin KG, Seguin F, Bastos DC, Agostini M, Rangel ALC, et al. Fatty acid synthase inhibition with Orlistat promotes apoptosis and reduces cell growth and lymph node metastasis in a mouse melanoma model. Int J Cancer. 2008; 123:2557–65. [PubMed: 18770866]
37. Hill TK, Davis AL, Wheeler FB, Kelkar SS, Freund EC, Lowther WT, et al. Development of a Self-Assembled Nanoparticle Formulation of Orlistat, Nano-ORL, with Increased Cytotoxicity against Human Tumor Cell Lines. Mol Pharm. 2016; 13:720–8. [PubMed: 26824142]
38. Hill TK, Abdulahad A, Kelkar SS, Marini FC, Long TE, Provenzale JM, et al. Indocyanine Green-Loaded Nanoparticles for Image-Guided Tumor Surgery. Bioconjug Chem. 2015; 26:294–303. [PubMed: 25565445]
39. Di Veroli GY, Fornari C, Wang D, Mollard S, Bramhall JL, Richards FM, et al. Combenefit: an interactive platform for the analysis and visualization of drug combinations. Bioinformatics. 2016; 32:2866–8. [PubMed: 27153664]
40. Chou TC. Drug combination studies and their synergy quantification using the chou-talalay method. Cancer Res. 2010:440–6. [PubMed: 20068163]
41. Zeisel SH, Niculescu MD. Perinatal choline influences brain structure and function. Nutr Rev. 2006; 64:197–203. [PubMed: 16673755]
42. Mebratu Y, Tesfaigzi Y. How ERK1/2 activation controls cell proliferation and cell death is subcellular localization the answer? Cell Cycle. 2009:1168–75. [PubMed: 19282669]
43. Lu Z, Xu S. ERK1/2 MAP kinases in cell survival and apoptosis. IUBMB Life. 2006; 58:621–31. [PubMed: 17085381]
44. Xiao D, Singh SV. Phenethyl isothiocyanate-induced apoptosis in p53-deficient PC-3 human prostate cancer cell line is mediated by extracellular signal-regulated kinases. Cancer Res. 2002; 62:3615–9. [PubMed: 12097262]
45. Ranganathan S, Benetatos CA, Colarusso PJ, Dexter DW, Hudes GR. Altered beta-tubulin isotype expression in paclitaxel-resistant human prostate carcinoma cells. Br J Cancer. 1998; 77:562–6. [PubMed: 9484812]
46. Bhardwaj A, Srivastava SK, Singh S, Arora S, Tyagi N, Andrews J, et al. CXCL12/CXCR4 signaling counteracts docetaxel-induced microtubule stabilization via p21-activated kinase 4-dependent activation of LIM domain kinase 1. Oncotarget. 2014; 5:11490–500. [PubMed: 25359780]
47. Ahmed AA, Wang X, Lu Z, Goldsmith J, Le XF, Grandjean G, et al. Modulating microtubule stability enhances the cytotoxic response of cancer cells to paclitaxel. Cancer Res. 2011; 71:5806–17. [PubMed: 21775522]
48. Zhuang SH, Hung YE, Hung L, Robey RW, Sackett DL, Linehan WM, et al. Evidence for microtubule target engagement in tumors of patients receiving ixabepilone. Clin Cancer Res. 2007; 13:7480–6. [PubMed: 18094432]
49. Yang PY, Liu K, Ngai MH, Lear MJ, Wenk MR, Yao SQ. Activity-based proteome profiling of potential cellular targets of orlistat - An FDA-approved drug with anti-tumor activities. J Am Chem Soc. 2010; 132:656–66. [PubMed: 20028024]
50. Gao X, Hannoush RN. Method for cellular imaging of palmitoylated proteins with clickable probes and proximity ligation applied to hedgehog, tubulin, and ras. J Am Chem Soc. 2014; 136:4544–50. [PubMed: 24588349]

51. Bollu LR, Katreddy RR, Blessing AM, Pham N, Zheng B, Wu X, et al. Intracellular activation of EGFR by fatty acid synthase dependent palmitoylation. Oncotarget. 2015; 6:34992–5003. [PubMed: 26378037]
52. Fiorentino M, Zadra G, Palescandolo E, Fedele G, Bailey D, Fiore C, et al. Overexpression of fatty acid synthase is associated with palmitoylation of Wnt1 and cytoplasmic stabilization of beta-catenin in prostate cancer. Lab Investig. 2008; 88:1340–8. [PubMed: 18838960]
53. Heuer T, Ventura R, Mordec K, Lai J, Fridlib M, Buckley D, et al. FASN Inhibition and Taxane Treatment Combine to Enhance Anti-tumor Efficacy in Diverse Xenograft Tumor Models through Disruption of Tubulin Palmitoylation and Microtubule Organization and FASN Inhibition-Mediated Effects on Oncogenic Signaling and Gene Expression. EBioMedicine. 2017; 16:51–62. [PubMed: 28159572]
54. Paulmurugan R, Bhethanabotla R, Mishra K, Devulapally R, Foygel K, Sekar TV, et al. Folate Receptor-Targeted Polymeric Micellar Nanocarriers for Delivery of Orlistat as a Repurposed Drug against Triple-Negative Breast Cancer. Mol Cancer Ther. 2016; 15:221–31. [PubMed: 26553061]
55. Bhargava-Shah A, Foygel K, Devulapally R, Paulmurugan R. Orlistat and antisense-miRNA-loaded PLGA-PEG nanoparticles for enhanced triple negative breast cancer therapy. Nanomedicine. 2016; 11:235–47. [PubMed: 26787319]
56. Dolenc A, Govedarica B, Dreu R, Kocbek P, Srcic S, Kristl J. Nanosized particles of orlistat with enhanced in vitro dissolution rate and lipase inhibition. Int J Pharm. 2010; 396:149–55. [PubMed: 20540997]
57. Yang Y, Liu H, Li Z, Zhao Z, Yip-Schneider M, Fan Q, et al. Role of fatty acid synthase in gemcitabine and radiation resistance of pancreatic cancers. Int J Biochem Mol Biol. 2011; 2:89–98. [PubMed: 21331354]
58. Vazquez-Martin A, Ropero S, Brunet J, Colomer R, Menendez JA. Inhibition of Fatty Acid Synthase (FASN) synergistically enhances the efficacy of 5-fluorouracil in breast carcinoma cells. Oncol Rep. 2007; 18:973–80. [PubMed: 17786362]
59. Mims J, Bansal N, Bharadwaj MS, Chen X, Molina AJ, Tsang AW, et al. Energy metabolism in a matched model of radiation resistance for head and neck squamous cell cancer. Radiat Res. 2015; 183:291–304. [PubMed: 25738895]
60. Rae C, Haberkorn U, Babich JW, Mairs RJ. Inhibition of Fatty Acid Synthase Sensitizes Prostate Cancer Cells to Radiotherapy. Radiat Res. 2015; 184:482–93. [PubMed: 26484401]

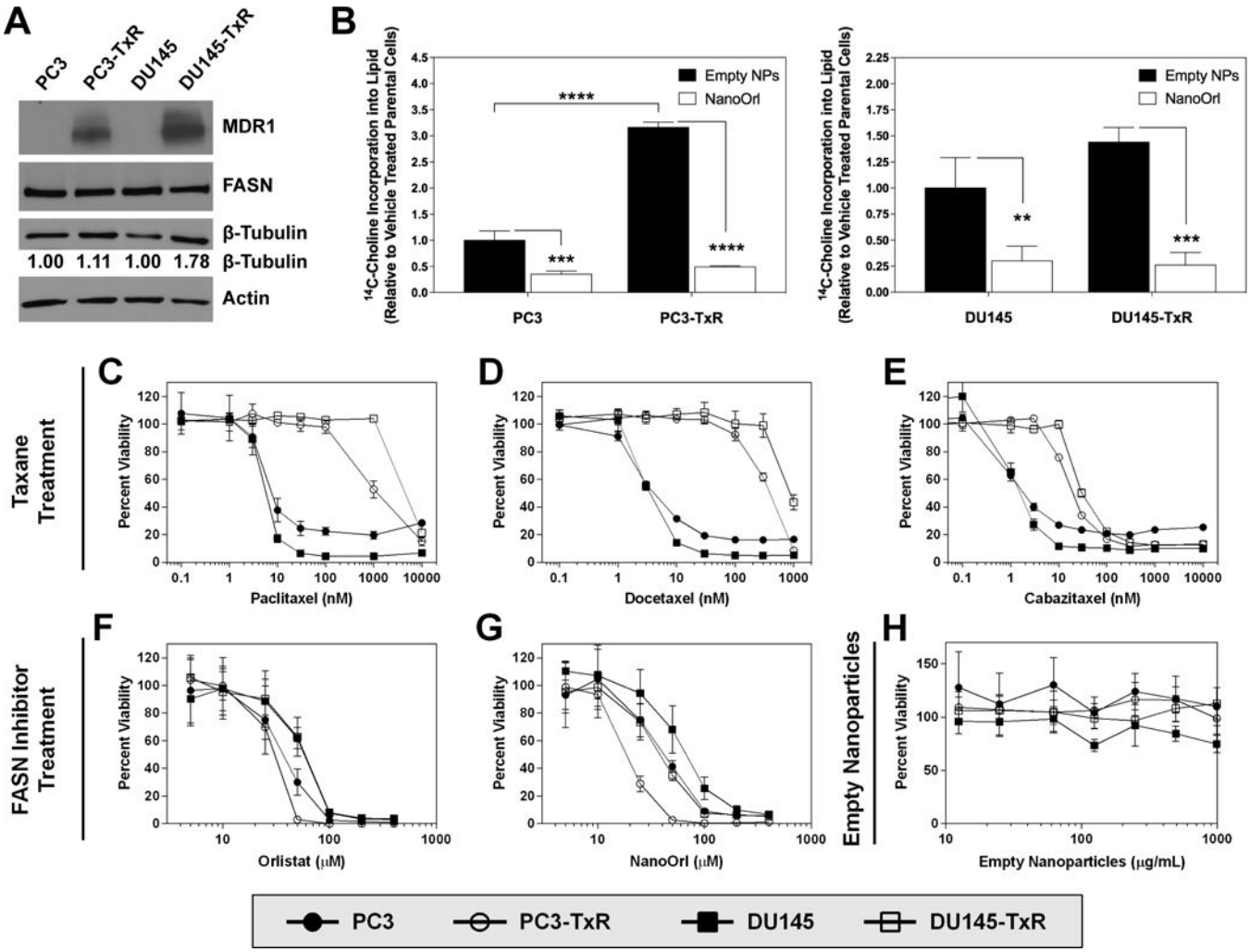

Figure 1. Confirmation of taxane-resistance and sensitivity to orlistat and NanoOrl

(A) Protein expression was assessed with immunoblot of whole-cell protein lysates. Quantification of β-tubulin levels is provided relative to parent cells. (**B)** Cells were treated with empty NPs or NanoOrl (50μM) for 24 h. Cells were pulsed with 1μCi [methyl-^{14}C]choline chloride for 2 h and ^{14}C-Choline incorporation into lipids was quantified by scintillation counting and normalized to protein concentration. Values are expressed as mean ± s.d. of three separate experiments. *$p < 0.05$, **$p < 0.01$, ***$p < 0.001$, ****$p < 0.0001$; as determined by ANOVA with Tukey's method for multiple comparison. **C–H**, Parent PC3 and DU145 or taxane-resistant PC3-TxR and DU145-TxR cells were treated with indicated concentrations of taxanes [paclitaxel **(C)**, docetaxel **(D)**, or cabazitaxel **(E)**], orlistat **(F)**, NanoOrl **(G)**, or empty nanoparticles **(H)**. $N = 6$ technical replicates per treatment. After 72 h, cell viability was assessed with the CCK-8 assay. Cell viability data was normalized to untreated control wells on each plate.

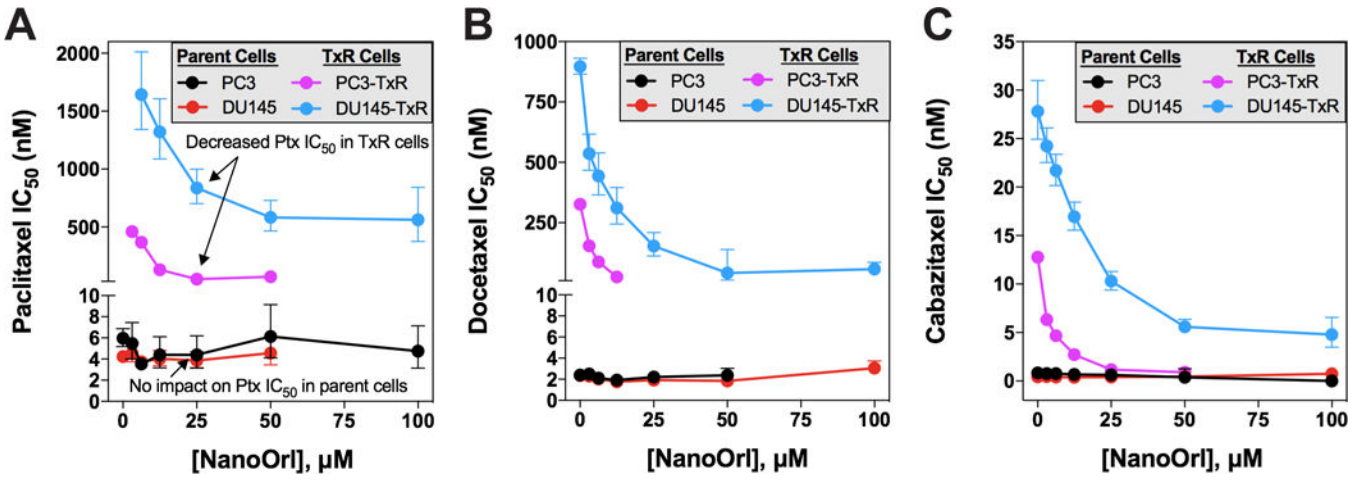

Figure 2. Nano-Orlistat decreases IC_{50} of taxanes in taxane-resistant prostate cancer cells

Parent PC3 and DU145 or taxane-resistant PC3-TxR and DU145-TxR cells were treated with combinations of 8 concentrations of **(A)** paclitaxel, **(B)** docetaxel, and **(C)** cabazitaxel with 7 concentrations of NanoOrl. $N = 6$ replicates per combination. After 72 h, cell viability was assessed with the CCK-8 assay. Each dot represents the calculated IC_{50} value of the indicated taxane as a function of NanoOrl concentration, with the error bars representing the 95% confidence interval. Some error bars are not visible due to the small range of 95% confidence interval.

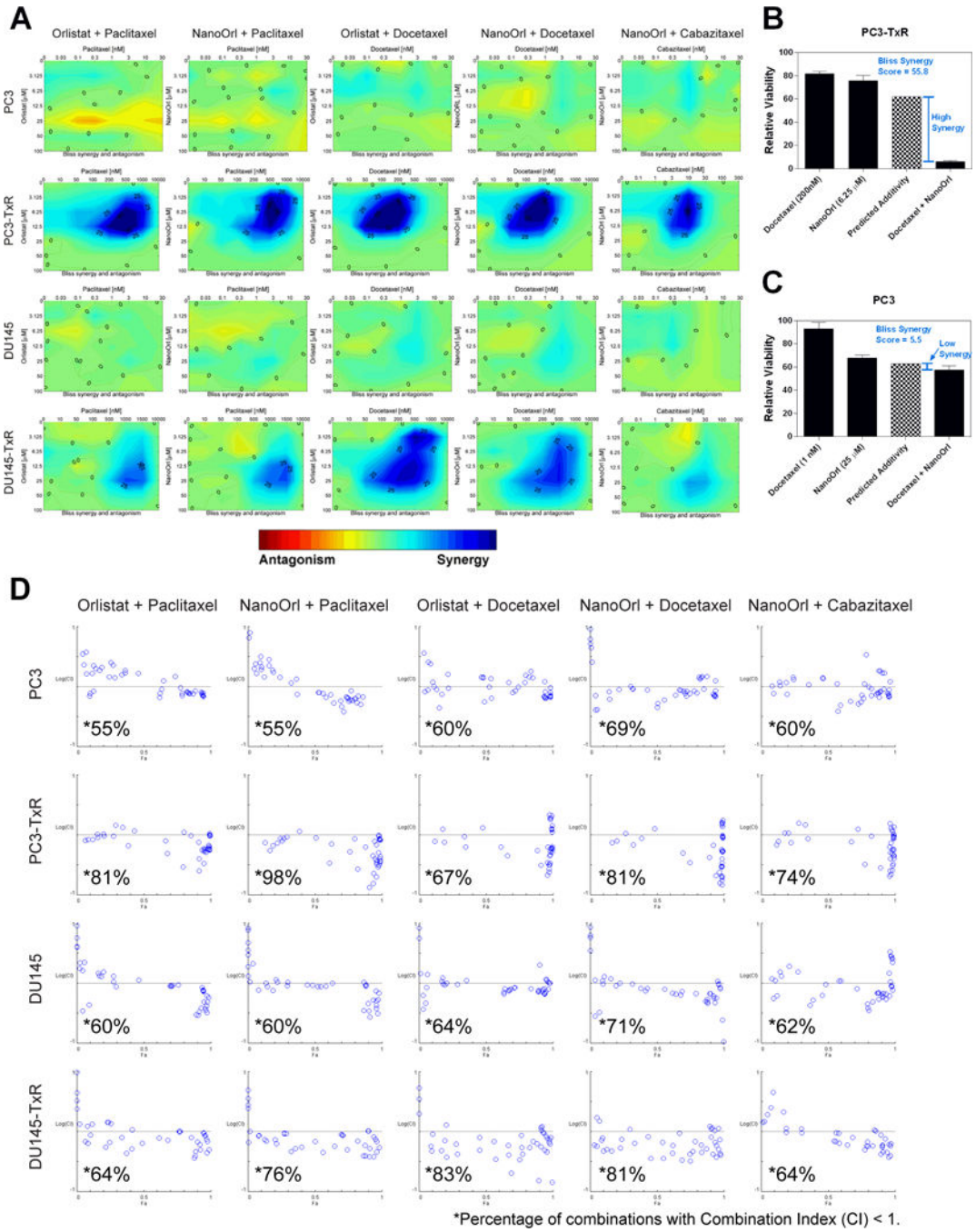

Figure 3. Combinations of orlistat or NanoOrl with taxanes are additive in parent cells, and synergistic in taxane-resistant cells

(A) Cells were treated as in Figure 2 with the indicated concentrations (taxane concentration above the x-axis, orlistat or NanoOrl concentration along the y-axis) and assessed with CCK-8 assay. Cell viability data was normalized to untreated control wells on each plate. Synergy was analyzed using Combenefit software. Results show the “Contour” view of synergy/antagonism calculations of synergy scores (the difference between the predicted additivity and the observed viability) for the Bliss model. Significant synergy is denoted by

dark blue areas, and areas with synergy scores above 25 and 50 are marked. Bar graphs show two examples of the observed single agent and combination relative viability (dark bars), and the predicted additivity (checkered bar) from the Bliss model for **(B)** PC3-TxR and **(C)** PC3 cells. **(D)** Cells were treated as in Figure 2 and 3A, and synergy of the normalized data was analyzed using CompuSyn software. Results show synergy/antagonism plotted as the Log(combination index) [Log(CI)] on the y-axis vs the Fraction affected (Fa) on the x-axis. Combinations with CI value <1 are synergistic and are plotted below the horizontal line, combinations with CI=1 are additive and are plotted on or near the horizontal line, and combinations with CI>1 indicates antagonism, and are plotted above the horizontal line. The percentage of combinations with CI < 1 for each cell line treated with the indicated drugs are marked with *.

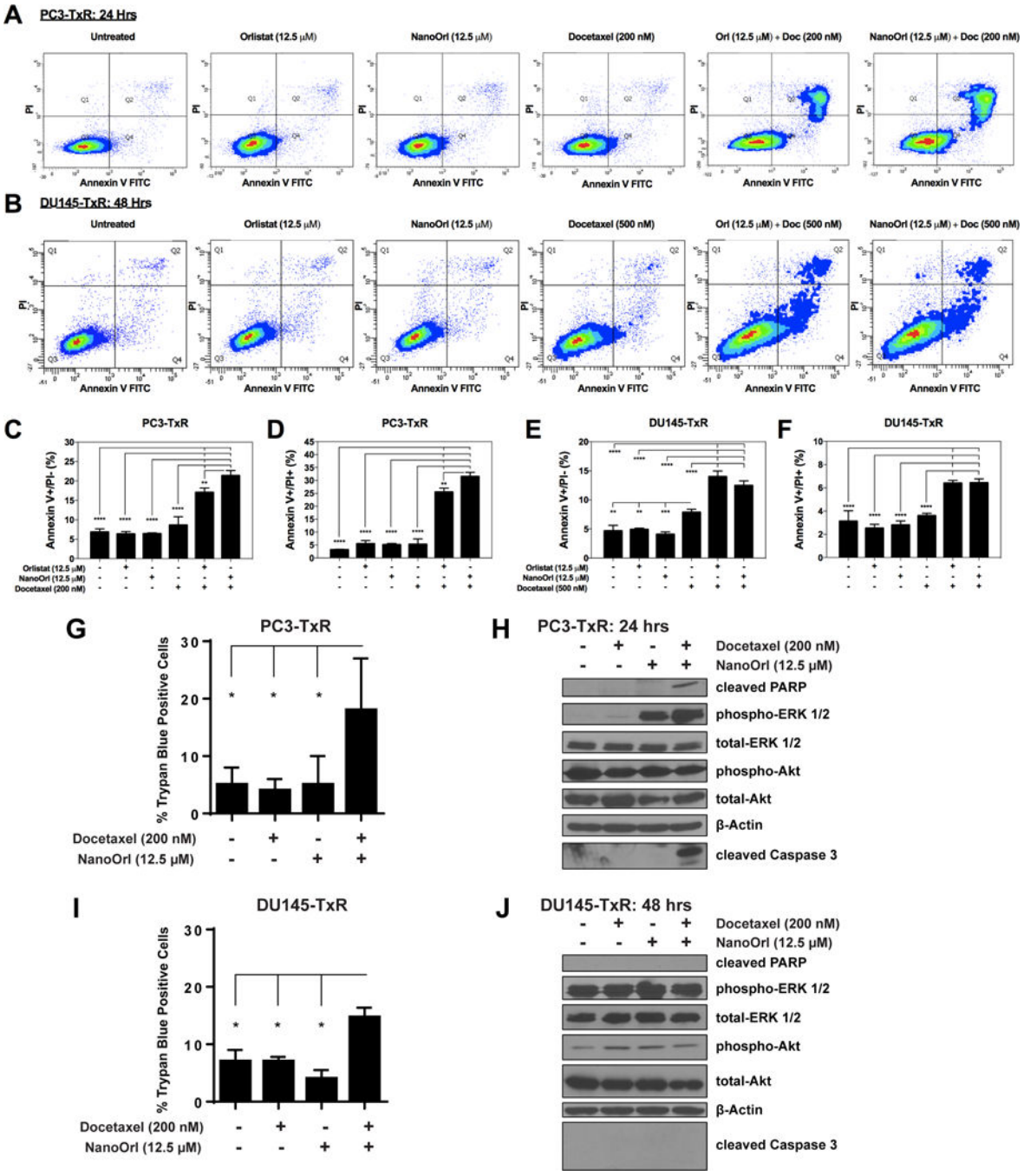

Figure 4. Combination of orlistat or NanoOrl plus docetaxel induce apoptosis

PC3-TxR **(A)** and DU145-TxR cells **(B)** were treated as indicated and stained with AnnexinV-FITC and Propidium Iodide (PI) using FITC Annexin V Apoptosis Detection Kit I (BD Biosciences), and quantified with flow cytometry. Representative scatter plots from each treatment are shown. **(C–F)** The percentage of early apoptotic (Annexin V+/PI-; **C and E**), and late apoptotic/necrotic (Annexin V+/PI+; **D and F**) cells are quantified (n = 3 technical replicates). Values are expressed as mean ± s.d. *p < 0.05, **p < 0.01, ***p < 0.001, ****p < 0.0001; as determined by ANOVA with Tukey's method for multiple

comparison. PC3-TxR cells (**G**) treated for 24 hours and DU145-TxR cells (**I**) treated for 48 hours with indicated treatments were counted in a hemocytometer by trypan blue exclusion using an Invitrogen CountessTM Automated Cell Counter. Values are expressed as mean ± s.d. P-values determined by a two-tailed Student's t-test. *p≤0.05. PC3-TxR **(H)** and DU145-TxR (**J**) cells were treated as indicated. Expression of the indicated proteins was analyzed by immunoblot.

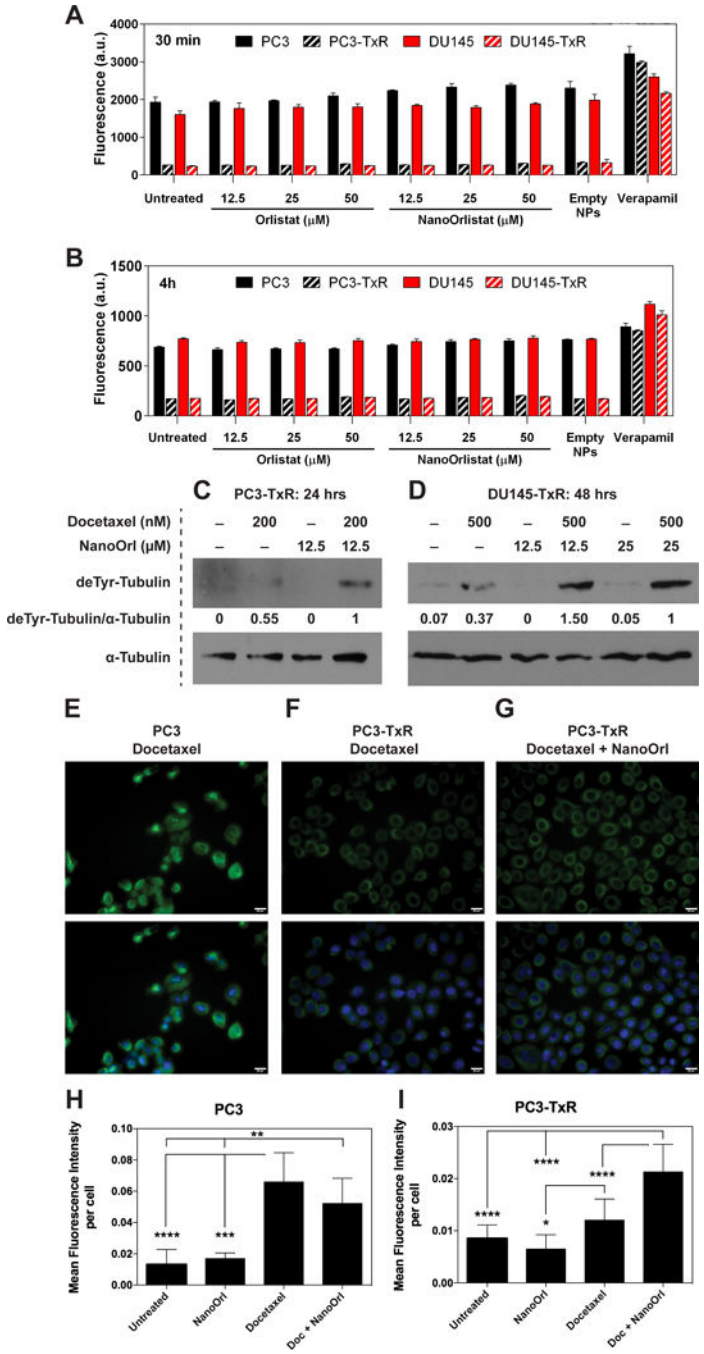

Figure 5. NanoOrl does not affect MDR1 activity, and combination of NanoOrl plus docetaxel stabilizes microtubules in taxane-resistant cells

MDR1 activity was assessed in cells with the Vybrant Multidrug Resistance Assay Kit (Thermo Fisher) after 30 min **(A)** or 4 h **(B)** of treatment with the indicated concentrations of orlistat or NanoOrl. Cells were also treated with empty nanoparticles (empty NPs, 0.124 mg/mL) or verapamil (50 μM), an MDR1 inhibitor, which was used as a positive control. After washing with PBS, the cell fluorescence was measured with a plate reader. Values are expressed as mean ± s.d. of n = 3 technical replicates. PC3-TxR **(C)** or DU145-TxR cells

(D) were treated as indicated. After washing with PBS, whole cell protein lysates were collected in RIPA buffer, quantified, and protein expression was assessed with immunoblot. deTyr-Tubulin = detyrosinated alpha tubulin (a.k.a. Glu-tubulin). The same lysates were run on a separate gel and probed with an antibody against α-Tubulin to check equal loading. The ratio of deTyr-Tubulin to α-Tubulin is given relative to combination treatment. PC3 **(E)** or PC3-TxR cells **(F and G)** were treated with 200 nM docetaxel (Doc), 12.5 μM NanoOrl, or the combination as indicated for 2.5 h. Cells were stained with anti-detyrosinated tubulin antibody (green), a marker of stabilized microtubules, and DAPI (blue). Scale bar = 20 μm. (**H–I)**, Quantification of the mean fluorescence intensity per cell ± s.d. of 10 areas from 2 separate wells is shown below. *p < 0.05, **p < 0.01, ***p < 0.001, ****p < 0.0001; as determined by ANOVA with Tukey's method for multiple comparison.

Table 1

IC_{50} values of PC3, PC3-TxR, DU145, and DU145-TxR Cells[a]

Drug	PC3	PC3-TxR	Fold Resistance[b]	DU145	DU145-TxR	Fold Resistance[b]
Paclitaxel (nM)	6.14 ± 0.91	941 ± 73	153	4.88 ± 0.47	2438 ± 309	500
Docetaxel (nM)	3.56 ± 0.36	383 ± 54	108	2.71 ± 0.25	912 ± 95	337
Cabazitaxel (nM)	1.19 ± 0.13	14.8 ± 1.1	12	0.79 ± 0.29	30.4 ± 2.8	39
Orlistat (μM)	30 ± 5.3	20 ± 6.1	0.67	46 ± 7.7	42 ± 9.5	0.92
NanoOrl (μM)	37 ± 8.6	16 ± 2.6	0.43	51 ± 6.6	39 ± 3.7	0.77

[a]Cells were treated for 72 h and cell viability was assessed with the CCK-8 assay (Dojindo, Japan). Table shows the mean IC_{50} ± SD of at least two independent experiments.

[b]Fold Resistance is the ratio of the IC_{50} in TxR cells relative to parental cells for the same drug. “NanoOrl (μM)” represents the equivalent concentration of orlistat and not the concentration of the NP.